

# Magnetospheric electrodynamics

## A generalized Grad-Shafranov solver



Jens F. Mahlmann, Prof. Miguel A. Aloy (CAMAP)

Universitat de València  
Departament d'Astronomia i Astrofísica

CoCoNut Meeting  
Valencia / December 16, 2016

# No clear picture from merger simulations

## Failing of jet launching despite favorable conditions

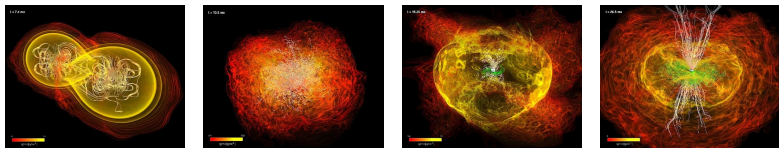


Figure: Simulation of the merger of two neutron stars (Rezzolla et al., 2011) with gravitational mass of 1.5 solar masses each during a time of 26.5 ms.

- Despite favorable conditions (e.g., magnetic fields) no jets clearly emerge after the BH formation (Rezzolla et al., 2011; Kiuchi et al., 2014). Simulations by Ruiz et al. (2016) did, however, discover jet launching.
- Possible explanations for missing jets: Short simulation time or *field reversals* observed over the low density funnel.

Current set of 'standard' magnetospheric field topologies (e.g., split-monopole, paraboloidal) may not be sufficient for time evolution simulations of the electromagnetic fields anymore.

# Blandford/Znajek explain jet powering I

## Creating a force-free black hole magnetosphere

Introduction

Force-free  
e-dynamics

Numerical  
strategies

Outlook

Open forum

References

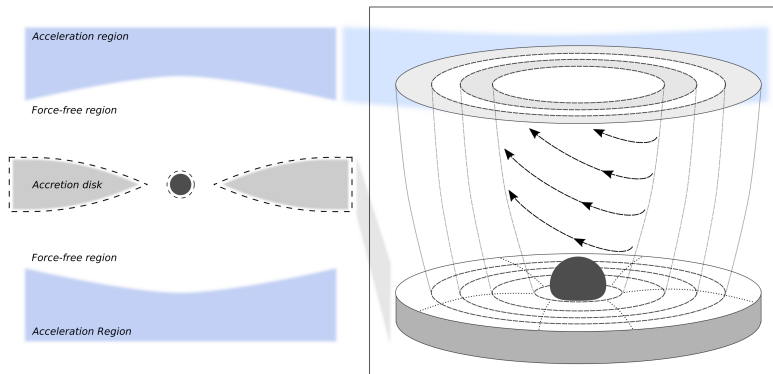


**Figure:** Schematic visualization of the Blandford/Znajek model (cf. MacDonald and Thorne, 1982). The black hole is embedded in a force-free magnetosphere. Magnetic fields are supported by a thin disc in the  $\theta = \pi/2$  equatorial plane. The acceleration region which involves a break-down of the idealized conditions is set up at infinity and not considered for the derivations. A non-degenerate plasma generation region is schematically represented by the dashed lines.

# Blandford/Znajek explain jet powering II

## Spacetime magnetospheric electrodynamics

Blandford and Znajek (1977) intensively exploit the *covariant* form of the Maxwell equations in Kerr spacetime.

$$(*F^{\mu\nu})_{;\nu} = 0$$

$$\varepsilon_0^{-1} J^\mu = F_{;\nu}^{\mu\nu} = g^{-1/2} \left( g^{1/2} F^{\mu\nu} \right)_{;\nu}$$

$$F_{\mu\nu} = \mathcal{A}_{\nu,\mu} - \mathcal{A}_{\mu,\nu}$$

The existence of time-like and axial-like *symmetries* help to reduce the complexity of the resulting equations.

$$\mathcal{A}_{\mu,t} = \mathcal{A}_{\mu,\phi} = 0$$

$$\implies F_{t\phi} = F_{\phi t} = 0$$

The *force-free condition* ultimately reduces to a differential equation governing the magnetosphere.

$$F_{\mu\nu} J^\nu = 0$$

$$4 \frac{\Sigma}{\Delta} l l' = - \left( \frac{\Sigma - 2Mr}{\Sigma \sin \theta} \Psi_{,r} \right)_{,r} - \left( \frac{\Sigma - 2Mr}{\Delta \Sigma \sin \theta} \Psi_{,\theta} \right)_{,\theta}$$

$$+ \omega^2 \left\{ \sin \theta \left( \frac{A}{\Sigma} \Psi_{,r} \right)_{,r} + \frac{1}{\Delta} \left( \frac{A \sin \theta}{\Sigma} \Psi_{,\theta} \right)_{,\theta} \right\}$$

$$- 4Maw \left\{ \sin \theta \left( \frac{r\Psi_{,r}}{\Sigma} \right)_{,r} + \frac{r}{\Delta} \left( \frac{\sin \theta}{\Sigma} \Psi_{,\theta} \right)_{,\theta} \right\}$$

$$+ \frac{\sin \theta}{\Sigma \Delta} (A\omega - 2Mar) \left( \Delta (\Psi_{,r})^2 + (\Psi_{,\theta})^2 \right) \omega'$$

- Second order non-linear elliptic PDE
- Singular surfaces (so called *light cylinders*)
- Mathematical treatment differs from the (analytical) approach in the neutron star case

## Solving GS as an elliptic PDE

## Numerical PDE solving routine with SOR scheme

The Grad-Shafranov equation is resolved into a *linear* part  $\mathcal{G}_l$  and the *non-linear* source terms  $\mathcal{G}_s$ .

$$\begin{aligned} \mathcal{G}_l = \omega^2 & \left\{ \sin \theta \left( \frac{A}{\Sigma} \Psi_{,r} \right)_{,r} + \frac{1}{\Delta} \left( \frac{A \sin \theta}{\Sigma} \Psi_{,\theta} \right)_{,\theta} \right\} \\ & - 4Maw \left\{ \sin \theta \left( \frac{r\Psi_{,r}}{\Sigma} \right)_{,r} + \frac{r}{\Delta} \left( \frac{\sin \theta}{\Sigma} \Psi_{,\theta} \right)_{,\theta} \right\} \\ & - \left( \frac{\Sigma - 2Mr}{\Sigma \sin \theta} \Psi_{,r} \right)_{,r} - \left( \frac{\Sigma - 2Mr}{\Delta \Sigma \sin \theta} \Psi_{,\theta} \right)_{,\theta} \\ \mathcal{G}_s = 4 \frac{\Sigma}{\Delta} I I' - \frac{\sin \theta}{\Sigma \Delta} (A\omega - 2Mar) & \left( \Delta (\Psi_{,r})^2 + (\Psi_{,\theta})^2 \right) \omega' \end{aligned}$$

- After discretization throughout the numerical grid,  $\mathcal{G}_l$  may be used as the linear operator in a numerical *PDE solving scheme* with non-linear sources  $\mathcal{G}_s$ .
- Following Contopoulos et al. (2013), a *SOR (successive overrelaxation)* method is employed for the relaxation procedure.

## Grad-Shafranov is not easily solved

The Contopoulos et al. (2013) strategy I

Contopoulos et al. (2013) suggest a simultaneous numerical treatment for the three functions  $\Psi$ ,  $\omega(\Psi)$  and  $I(\Psi)$  to solve the relativistic Grad-Shafranov equation:

- Discretize initial guesses for all physical quantities on a  $256 \times 64$  numerical grid:

$$\Psi(R, \theta) = 1 - \cos \theta \quad (\text{Pulsar potential})$$

$$\omega(\Psi) = 0.5 \Omega_{BH} \quad (\text{Ideal condition})$$

$$I(\Psi) = -0.5 \omega(\Psi) \Psi (2 - \Psi) \quad (\text{Pulsar potential})$$

$\omega(\Psi)$  and  $I(\Psi)$  are stored in functional tables accessed through interpolation.

- Use a *successive overrelaxation (SOR)* method to update  $\Psi$ . Boundaries set to Dirichlet in  $\theta$  and Neumann in  $r$ .

# Numerics at the light cylinders I

## Close-up: Understanding the singular surfaces

Field quantities of the  $3+1$  decomposition (as measured by the **ZAMOs**) are required to stay finite. Lee et al. (2000) derive the following:

$$\rho = \left( \frac{\Omega - \omega}{4\pi^2 \alpha} \right) \frac{\frac{8\pi^2 I}{\alpha^2} \frac{dI}{d\Psi} - \mathbf{G} \cdot \nabla \Psi}{D}$$

$$\mathbf{j}_T = \left( \frac{1}{4\pi^2 \varpi} \right) \frac{\frac{8\pi^2 I}{\alpha^2} \frac{dI}{d\Psi} - \left( \frac{\Omega - \omega}{\alpha} \varpi \right)^2 \mathbf{G} \cdot \nabla \Psi}{D}$$

where  $D$  denotes the light cylinder condition

$$D = 1 - \frac{(\omega - \Omega)^2 \varpi^2}{\alpha^2}.$$

Smoothness of  $\Psi$  throughout the magnetosphere is imposed as a regularity condition (as also used in, e.g., Contopoulos et al., 2013).

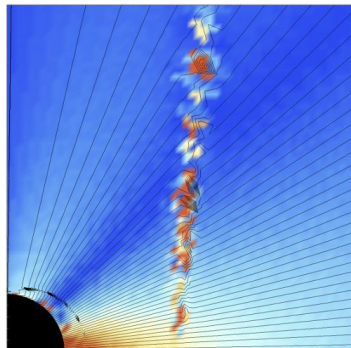


**Figure:** Numerical artifacts develop at the singular surfaces of the Grad-Shafranov equation (exaggerated). These breakings of field lines may cause the numerical solution to blow up.

**Strategy outline:** Ensure smooth passing through the light cylinders and reconstruct potential functions consistently.

# Grad-Shafranov is not easily solved

## The Contopoulos et al. (2013) strategy II

Introduction

Force-free  
e-dynamicsNumerical  
strategies

Outlook

Open forum

References

- Every other iteration, impose *weighted corrections* to  $\omega$  and  $I$  according to the non-smoothness of  $\Psi$  at the light cylinders (singular surfaces of the GS-equation). Update scheme according to:

$$\begin{aligned}\Psi_{new} &= 0.5 \cdot [\Psi_{LC}^+ + \Psi_{LC}^-] \\ \omega(\Psi_{new}) &= \omega(\Psi_{old}) + \mu_\omega \cdot [\Psi_{LC}^+ - \Psi_{LC}^-] \\ I(\Psi_{new}) &= I(\Psi_{old}) + \mu_I \cdot [\Psi_{LC}^+ - \Psi_{LC}^-]\end{aligned}$$

$\Psi_{LC}^+$  and  $\Psi_{LC}^-$  refer to the extrapolated potential lines at the light cylinder. The numerical parameters are derived empirically and depend on the setup.

- Additional *polynomial data fitting* (order determined empirically) is applied to the functions  $\omega(\Psi)$  and  $I(\Psi)$ .
- A relaxed state is said to be reached after  $\sim 5000$  iterations.



# Numerics at the light cylinders II

## Close-up: Relaxation and smoothing procedures

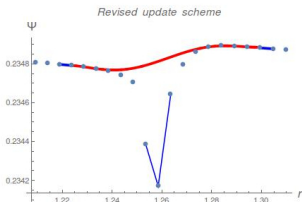


Figure: Visualization of the smoothing scheme applied at the light cylinders.

The Grad-Shafranov equation may be studied on the singular surfaces after the smoothing procedure:

$$4 \frac{\Sigma}{\Delta} II' = \mathcal{G}S_{LC}$$

$$+ \mathcal{G}S_D \cdot \left[ \frac{\omega^2 A \sin^2 \theta}{\Sigma} - \frac{4Mar\omega \sin^2 \theta}{\Sigma} - 1 + \frac{2Mr}{\Sigma} \right]$$

At the location of the light cylinders, a simplified equation can be solved (cf. Uzdensky, 2004) in order to relate the defining functions  $\mathcal{A}_\phi$ ,  $\omega$  and  $I$ .

### Simultaneous relaxation of $\omega$ and $II'$

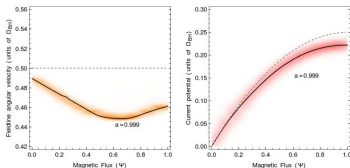


Figure: Numerical solution of the Grad-Shafranov (spin parameter  $a = 0.9999$ ). *Colored shading*: Location of the functions throughout the numerical procedure.

### Separate relaxation of $\omega$ or $II'$

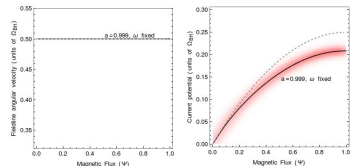


Figure: Numerical solution of the Grad-Shafranov (spin parameter  $a = 0.9999$ ). *Colored shading*: Location of the functions throughout the numerical procedure.

# Make use of Grad-Shafranov solutions

## Construction of initial data for time evolution

Introduction

Force-free  
e-dynamics

Numerical  
strategies

Outlook

Open forum

References

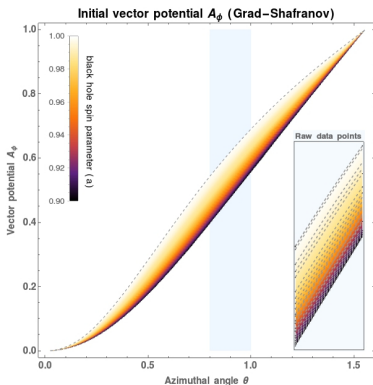


Figure: Visualization of the *vector potential* as a solution of the Grad-Shafranov equation for a *field line angular velocity*  $\omega$  fixed to  $\Omega_{BH}/2$  and black hole *spin parameters* between  $a = 0.9$  and  $a = 0.9999$ . The data points used for interpolation are depicted in the bottom left. (Grad-Shafranov solver,  $2 \cdot 10^6$  iterations)

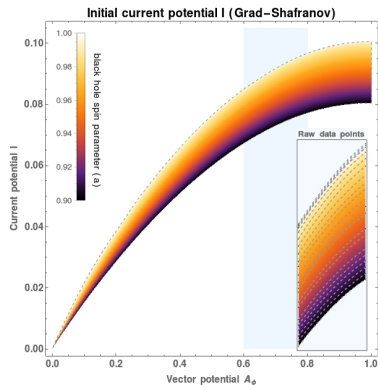


Figure: Visualization of the *current potential* as a solution of the Grad-Shafranov equation for a *field line angular velocity*  $\omega$  fixed to  $\Omega_{BH}/2$  and black hole *spin parameters* between  $a = 0.9$  and  $a = 0.9999$ . The data points used for interpolation are depicted in the bottom left. (Grad-Shafranov solver,  $2 \cdot 10^6$  iterations)



## Open forum: Let's discuss

Questions. Answers. Remarks. Discussion.

**Thank you.**



European Research Council  
Established by the European Commission



Studienstiftung  
des deutschen Volkes

## References I

- R. D. Blandford and R. L. Znajek. Electromagnetic extraction of energy from Kerr black holes. *Monthly Notices of the Royal Astronomical Society*, 179(3):433–456, 1977. doi: 10.1093/mnras/179.3.433.
- I. Contopoulos, D. Kazanas, and D. B. Papadopoulos. The force-free magnetosphere of a rotating black hole. *The Astrophysical Journal*, 765(2):113, 2013. doi: 10.1088/0004-637x/765/2/113.
- K. Kiuchi, K. Kyutoku, Y. Sekiguchi, M. Shibata, and T. Wada. High resolution numerical relativity simulations for the merger of binary magnetized neutron stars. *Phys. Rev. D*, 90(4), 2014. doi: 10.1103/physrevd.90.041502.
- H. K. Lee, R. Wijers, and G. Brown. The Blandford-Znajek process as a central engine for a gamma-ray burst. *Physics Reports*, 325(3):83–114, 2000. doi: 10.1016/s0370-1573(99)00084-8.
- D. MacDonald and K. S. Thorne. Black-hole electrodynamics: an absolute-space/universal-time formulation. *Monthly Notices of the Royal Astronomical Society*, 198(2):345–382, 1982. doi: 10.1093/mnras/198.2.345.
- L. Rezzolla, B. Giacomazzo, L. Baiotti, J. Granot, C. Kouveliotou, and M. A. Aloy. The missing link: Merging neutron stars naturally produce jet-like structures and can power short gamma-ray bursts. *The Astrophysical Journal*, 732(1):L6, 2011. doi: 10.1088/2041-8205/732/1/L6.
- M. Ruiz, R. N. Lang, V. Paschalidis, and S. L. Shapiro. Binary neutron star mergers: A jet engine for short gamma-ray bursts. *The Astrophysical Journal*, 824(1):L6, 2016. doi: 10.3847/2041-8205/824/1/L6.
- D. A. Uzdensky. Force-free magnetosphere of an accretion disk - black hole system. I. schwarzschild geometry. *The Astrophysical Journal*, 603(2):652–662, 2004. doi: 10.1086/381543.